17th World Conference on Earthquake Engineering, 17WCEE
Sendai, Japan - September 13th to 18th 2020

SEISMIC PERFORMANCE OF COKE SLIT DAMPER WITH MULTIPLE PLASTIC ZONES

R.W. Alemayehu [1], J.H. Bae [2], C.H. Lee [3], M.J. Park [4], Y.S.Kim [5], J.H.Ryu [6], Y.K. Ju [7]

[1] *Ph.D. candidate, Korea University, Robel@korea.ac.kr*
[2] *Research Professor, Korea University, skycitykorea@gmail.com*
[3] *Professor, Pukyong National University, chlee@pknu,.ac.kr*
[4] *Ph.D. candidate, Korea University, alswo87039@korea.ac.kr*
[5] *CEO, TechSquare, yskim@techsq.co.kr*
[6] *Senior Researcher, TechSquare, jryu@techsq.co.kr*
[7] *Professor, Korea University, tallsite@korea.ac.kr*

Abstract

Metallic strip dampers are among the most widely used passive energy dissipation devices used for wind and earthquake control. As the height to width ratio of metallic strip dampers increases, the bending behavior becomes more dominant than the shear behavior. By taking this into account, a strip damper geometry named Coke slit damper is proposed. The Coke slit damper is proportioned following the moment gradient that results in a two end fully fixed and angularly distorted strip damper. The geometry of the coke slit damper is obtained by setting the flexural capacity of the strip to be equal to the moment demand at preselected segments to produce multiple plastic hinges simultaneously. Coke slit dampers that produce two, four, and infinite plastic zones per strip are studied by finite element analysis and cyclic load test. For the cyclic load test, FEMA incremental cyclic loading protocol is adapted. The studied parameters include energy dissipation capacity, stiffness, equivalent viscous damping ratio, failure mode, and behavior under fatigue load. The results show that all tested configurations of the damper have a stable hysteresis response with excellent energy dissipation capacity and ductility. Moreover, plastic hinges are developed at the intended locations at small angular distortion. As a result, energy dissipation is expected to start early in an earthquake. The structural characteristics of the device are readily determined from fundamental engineering principles; thus, the design can be easily modified or extended to suit structural requirements.

Keywords: Strip damper; Energy dissipation device; Passive control system; Reduced section; Cyclic load

1. Introduction

Structural control systems have gained popularity for their ability to reduce structural vibration. Passive, active, and semi-active control devices are widely used in new structures and retrofitting of existing structures [1,2]. Among all categories of structural control systems, passive control systems are the most popular [3-8]. Their effectiveness, inexpensiveness, and ability to function without external power source contribute to their popularity. One type of passive control device first proposed in the 1970s [9] and widely studied and implemented is the metal strip damper. Several researchers have studied different geometric configurations of metallic strip dampers to maximize energy dissipation and inelastic deformation. Tyler [10] proposed a tapered cantilever shape that utilizes the steel material's out of plane plastic deformation capacity. Pinelli et al. [11] proposed an inplane deforming steel damper based on a rectangular steel tube cut into a tapered shape such that the stresses distribute uniformly along with the tapered shape. Lee et al. [12] proposed a two side tapered steel strip that results in full-length yielding of two sides fixed and angularly distorted strip dampers.

In this paper, a non-uniform steel strip damper configuration named Coke slit damper is studied. The Coke slit damper results in multiple plastic hinges per strip. Comparison of the Coke slit damper with the full-length yielding damper of Lee et al. [12] is also made. The Coke slit damper showed stable hysteretic behavior and excellent cyclic performance.

2. Radius cut Coke shaped strip damper

When a two ends fixed strip damper is subjected to a horizontal in-plane force, bending moment and shear force co-occur. As the strip length to width ratio (aspect ratio) increases, bending becomes more dominant than shear. Taking this into account, Lee et al. [12] proposed a strip shape for strips with an aspect ratio of five or more. The proposed strip shape follows the bending moment gradient. The bending moment that results in a two end fixed strip can be visualized by simplifying the strip as a two end fixed beam with relative end displacement, as shown in Fig.1. In this loading condition, the strip deforms in double curvature, and the bending moment varies linearly with maximum moments at the ends and zeros out at the mid-segment, as shown in Fig.1. The resulting maximum moment is designated as M_1, and the moment at location *x* distance from the center (M_x) is calculated as shown in Fig.1.

To maximize the plastic zone and the plastic energy dissipation of the strip damper, the strip width is adjusted following the demand moment gradient shown in Fig.1. The moment capacity of each strip at any distance *x* from the center is set to be equal to the demanded moment, M_x, at the same location. In order to achieve this, the strip width (b_x) is parabolically tapered, while the strip thickness (t_x) is kept constant. At the mid-segment of the strip, the width of the strip is determined by considering the resulting shear force and membrane force [12]. The resulting shape is presented in Fig. 1 in red dotted line.

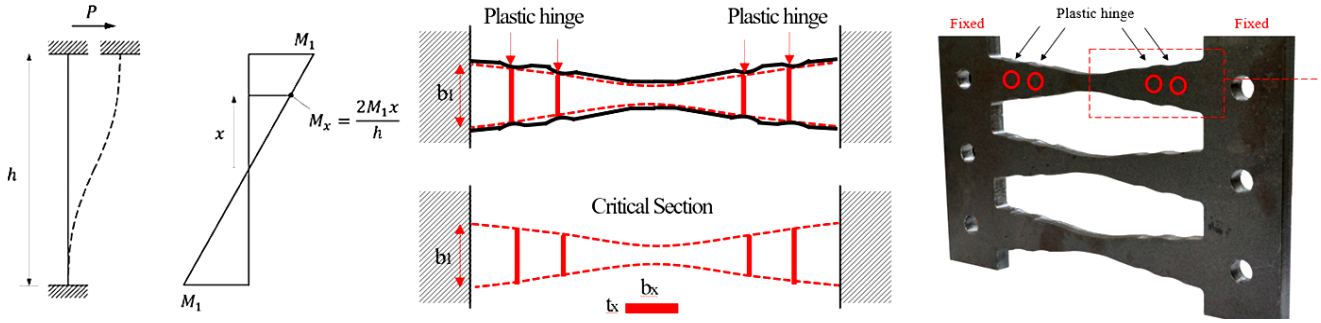

Fig. 1 – Moment distribution and configuration of Coke slit damper

The Coke shaped strip damper is obtained by modifying the full-length yielding strip damper to develop plastic hinges at pre-selected segments only. The coke shape strip with four plastic hinges is shown in the solid black line of Fig.1. As can be seen in Fig.1, the width of the Coke strip damper is increased from the full length yielding strip damper to result in a 20% plastic moment increase at all segments except at pre-selected four segments. The section at the pre-selected four segments is not increased to develop only four plastic hinges. A smooth circular curve provides a smooth transition from the broader segments to the plastic hinge regions.

3. Finite element study

3.1 Finite element models

The full length yielding strip damper and two Coke slit dampers with two and four plastic hinges per strip are studied through finite element analysis and cyclic loading test. In this paper, the emphasis is given to the finite element study. Fig. 2 shows the geometric details of the specimens. All the specimens have a length to width ratio of more than five in order to have flexure dominant behavior. The behavior of the three specimens under cyclic loading is studied through the nonlinear finite element analysis program Abaqus [13].

The incremental cyclic load specified in FEMA 461 [14] is adapted with a target displacement of 62mm. The ratio of loading amplitudes in successive loading steps is set to be 1.4, as suggested by [14]. The amplitude of the force step is designed to reach the target displacement at the fourteenth loading amplitude. In the first three loading step amplitudes, six cycles are applied at each loading amplitude. Starting from the

© The 17th World Conference on Earthquake Engineering

fourth loading amplitude, two cycles per loading amplitude are applied until the loading amplitude reaches the target displacement. Once the loading amplitude reaches the target displacement, loading at constant amplitude is continued until failure or strength degradation occurs. The finite element analysis is terminated at the loading cycle, where strength degradation occurred during the experiment.

The finite element is modeled using yield stress, ultimate stress, and Young's modulus of 341Mpa, 515 Mpa, and 176 Gpa, respectively. These mechanical properties are adapted from a coupon test carried out on the material of the strip damper. The stress-strain relation obtained from the coupon test is converted to true stress-true strain and assigned to the finite element models. The finite element models are meshed using an eight-node linear brick element with reduced integration. The average mesh size used to mesh the finite element models is 4 mm.

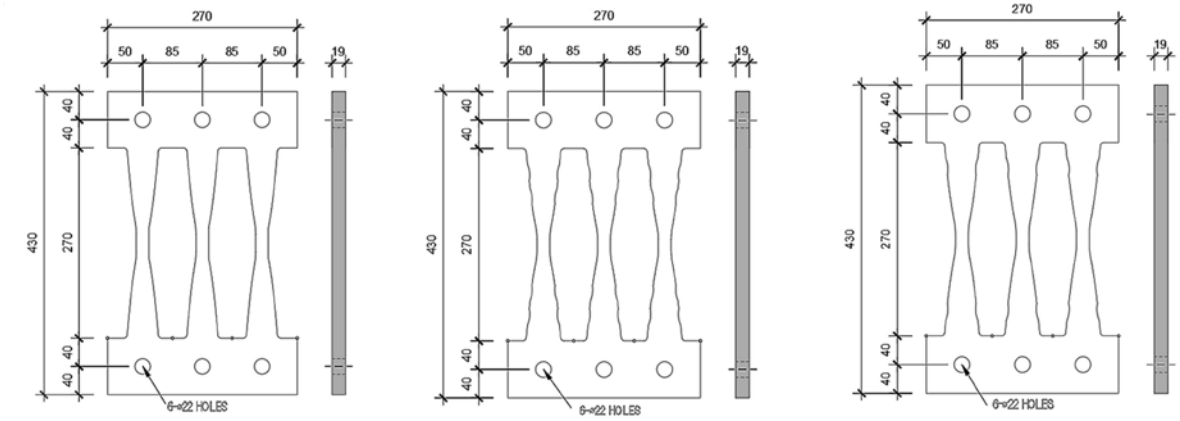

a. Continuous hinge (M_p) b. Four hinges (Coke 4) c. Two hinges (Coke 2)

Fig. 2 – Geometric details of finite element models

3.2 Verification of finite element model

The accuracy of the finite element model is examined by comparing the analysis result with the experimental results. The comparison is presented in the graphs of Fig.3. As can be seen from the graphs, the loading, unloading, and post yielding stiffnesses from the experiment and analysis are in good agreement. Moreover, the maximum forces in each cycle are in good agreement except where bolt sleeps occurred during the experiment.

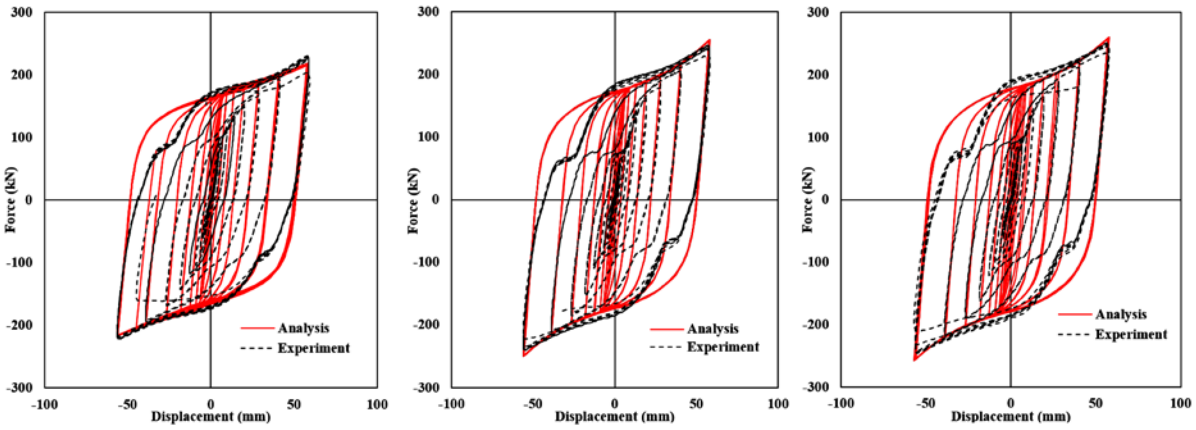

a. Continuous hinge (M_p) b. Four hinges (Coke 4) c. Two hinges (Coke 2)

Fig. 3 – Load deformation curve

© The 17th World Conference on Earthquake Engineering

4. Discussion of results

4.1 Load displacement relationship

Fig.3 shows the hysteresis curve of the three finite element models along with the experimental results. As can be seen from the graphs, all the three models show stable hysteresis up to the target displacement. Once the displacement reaches the target displacement, the cyclic loading is continued at a constant amplitude equal to the target displacement until strength degradation or rupture occurred. The finite element analysis is likewise continued until the cycle that caused strength degradation in the experiment. The cumulative displacement until the failure cycle for the M_p Coke-2, and Coke-4 models is 3092mm, 2437mm, and 2350mm, respectively. The full-length yielding specimen (M_p) survived nine cycles at the target displacement wile Coke-2 and Coke-4 survived six cycles at the target displacement. In all the three specimens, strength loss is initiated by cracks that lead to ductile fracture at the strip ends.

4.2 Stiffness, ductility, and strength

The structural characteristics are derived from the skeleton curve plotted by connecting the maximum loading points in each cycle. The skeletal curve shows a near bilinear curve, shown in Fig.4. From the bilinear curve, the initial stiffness is calculated as the slope of the elastic region. The post-yield stiffness is calculated as the slope of the post-yield load-deformation curve. The yield displacement is taken as the displacement that resulted in the first non-zero plastic strain in the finite element analysis. Table. 1 shows the values of these parameters computed from the skeleton curve.

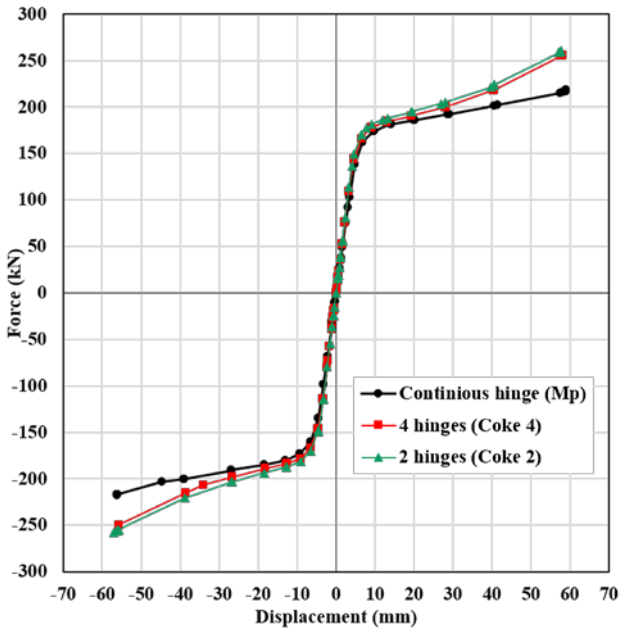

Fig. 4 – skeleton curve

The ductility and cumulative displacement are calculated as the ratio of the maximum displacement to the yield displacement and the summation of total displacements in each cycle. As can be seen from Table.1 and the skeleton curve of Fig.4, all the three specimens reached the target displacement without strength degradation. However, the Coke models started yielding at a smaller displacement compared to the full-length yielding (M_p) model. The early yield initiation led to a slightly higher ductility for the Coke 4 model compared to the other two models.

The full-length yielding (M_p) model showed smaller yield force, yield displacement, and post-yield stiffness due to the strip width difference. Coke 2 and Coke 4 behaved similarly with slightly higher forces

© The 17th World Conference on Earthquake Engineering

and stiffness in the Coke 2 model due to the relatively less number of plastic hinges on the Coke 2 model compared to the Coke 4 model.

Table 1 – Summary of ductility, strength, and stiffness

Model	Initial stiffness (kN/mm)	Yield force (kN)	Max force (kN)	Yield displacement (mm)	Max displacement (mm)	Ductility	Cumulative Displacement (mm)	Post yield stiffness (kN/mm)
M_p	30.22	102.6	218.7	3.40	58.95	17.36	3092.0	0.86
Coke 2	33.93	113.9	255.6	3.36	58.04	17.28	2437.4	1.62
Coke 4	34.74	113.9	260.5	3.28	57.74	17.60	2350.0	1.63

4.3 Energy dissipation

Fig.5 shows the cumulative dissipated energy calculated as the summation of the loop area of the load-displacement hysteretic curve up to the failure cycle. During the initial cycles where the inelastic deformation is zero or low, the cumulative dissipated energy is near zero.

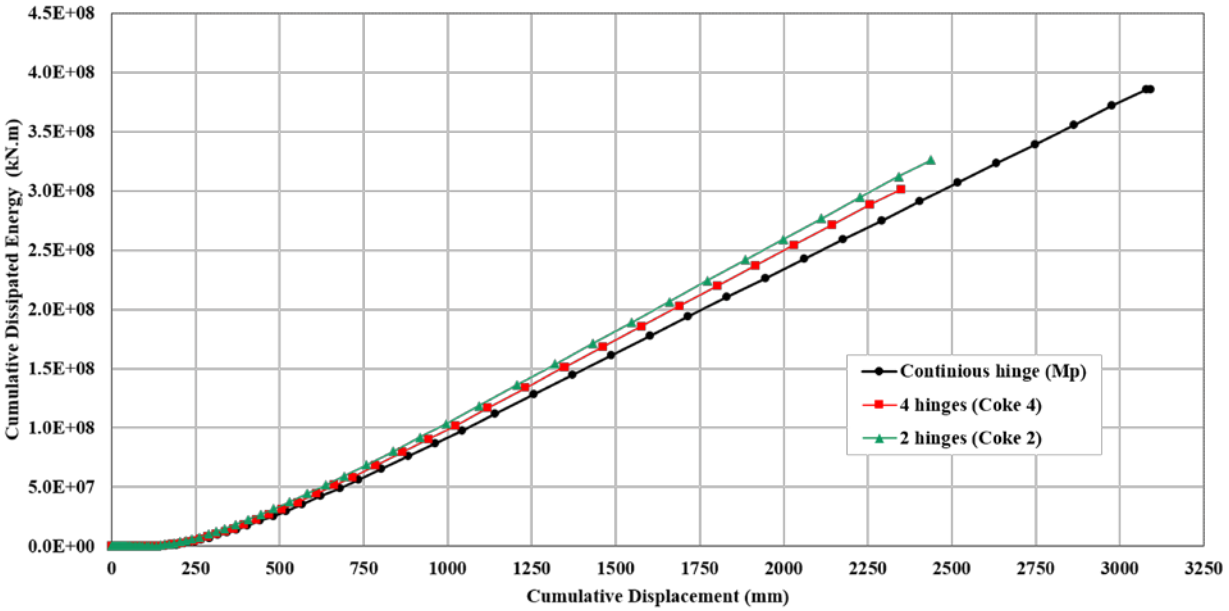

Fig. 5 – Cumulative dissipated Energy

The cumulative dissipated energy of the full-length yielding model (M_p) is lower than the Coke models at all values of cumulative displacement. However, since the M_p model sustained more cycles before failure, the total cumulative dissipated energy by the M_p model is higher than the Coke models.

4.4 Effective stiffness and equivalent damping

Metallic dampers dissipate energy through plastic deformation. The energy dissipation capacity is dependent on displacement. For displacement dependent dampers, effective stiffness and effective damping are used to describe the nonlinear properties of displacement dependent devices [15]. The effective stiffness is calculated by Eq. (1)

© The 17th World Conference on Earthquake Engineering

$$k_{\text{eff}} = \frac{|P_{\max}| - |P_{\min}|}{|\delta_{\max}| - |\delta_{\min}|} \tag{1}$$

Where P_{max}, P_{min}, δ_{max}, and δ_{min} represent the maximum force, minimum force, maximum displacement, and minimum displacement of a loading cycle, respectively. The force resistance at a displacement δ can be calculated by multiplying δ by the corresponding effective stiffness (K_{eff}).

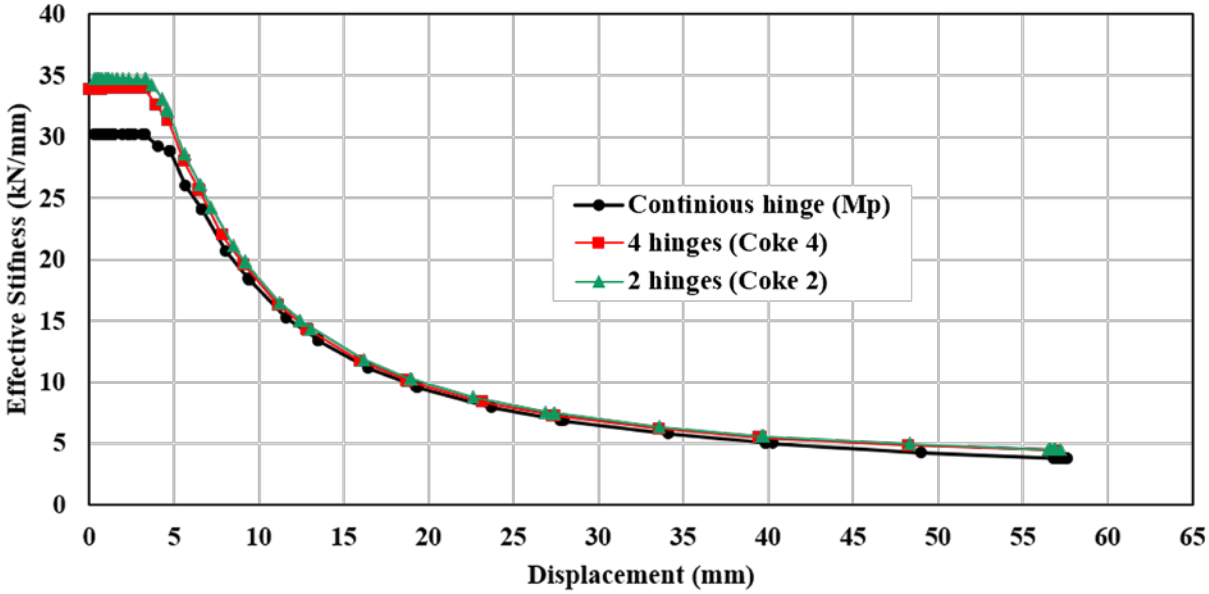

Fig. 6 – Effective stiffness

The effective damping β_{eff} and equivalent viscous damping ξ_{eq} characterize the energy dissipation capacity and are given by Eq. (2) and Eq.(3), respectively.

$$\beta_{eff} = \frac{2}{\pi} \frac{E_{loop}}{K_{eff}(|\delta_{max}| - |\delta_{min}|)^2} \tag{2}$$

$$\xi_{eq} = \frac{1}{4\pi} \frac{E_{loop}}{E_{so}} \tag{3}$$

Where E_{loop} is the area in one hysteresis cycle loop, and E_{so} is the stored energy. From the finite element analysis result, the variation of the effective stiffness, equivalent damping, and equivalent viscous damping is presented in Fig.6 to Fig. 8. The effective stiffness is constant before yielding, whereas the effective damping and equivalent damping are zero before yielding. After yielding, the effective stiffness of the three specimens decreases and merges, reaching a minimum effective stiffness of 2.4 kN/mm at the target displacement.

The equivalent damping and discous damping varies in a similar manner with displacement. At displacement levels ranging from 5mm to 27mm, the damping parameters of the full-length yielding strip damper is less than that of the Coke models. However, at large displacements, the equivalent and viscous damping parameters of the full-length yielding model is higher than that of the Coke shaped models. For intermediate displacement values ranging from 27mm to 40mm, the damping parameters of all the three models are identical.

© The 17th World Conference on Earthquake Engineering

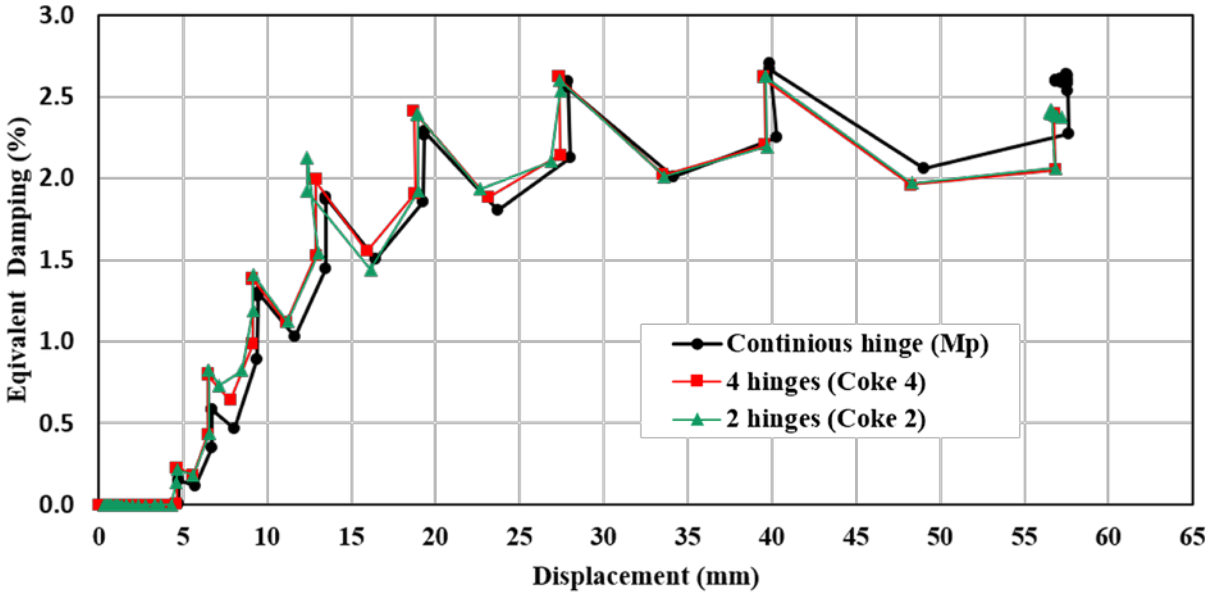

Fig. 7 – Equivalent Damping

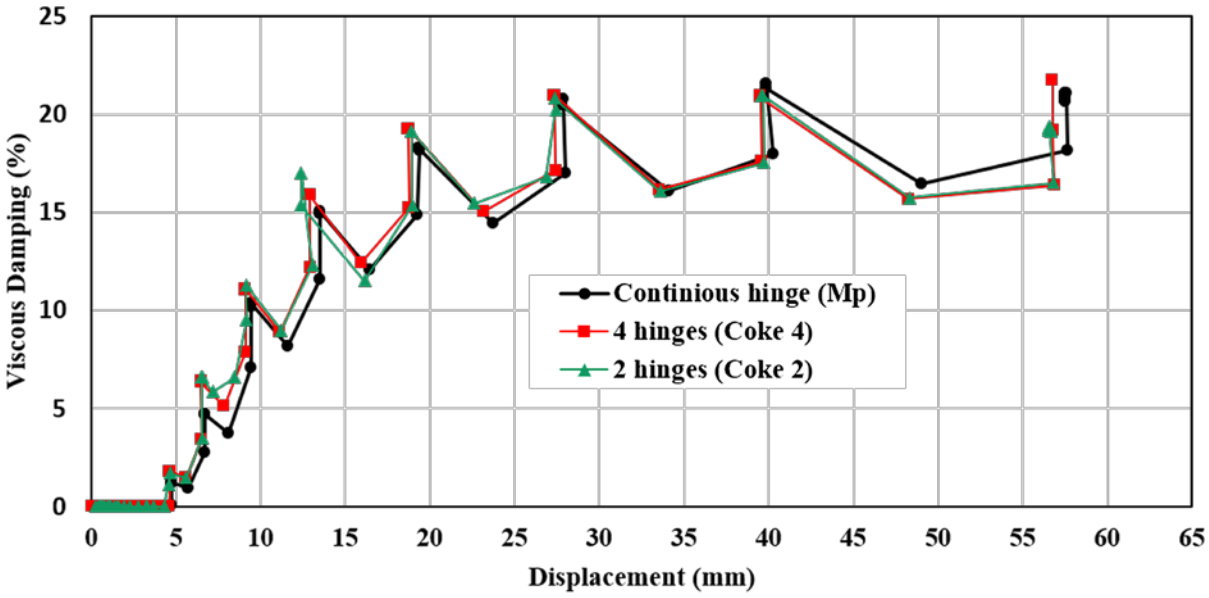

Fig. 8 – Viscous Damping

4.5 Stress distribution

Fig.9 shows the stress distribution at the target displacement. Consistent with the proportioning philosophy adopted, higher stresses are visible at the radius cuts of the coke shape strips. Similarly, the full-length yielding strip damper shows near-uniform stress distribution throughout the strip length with stress concentrations at the ends. The Coke shape strip models exhibited higher stress at the midsection due to the increased shear force resulting from the increase in the maximum force of the Coke slit dampers.

© The 17th World Conference on Earthquake Engineering

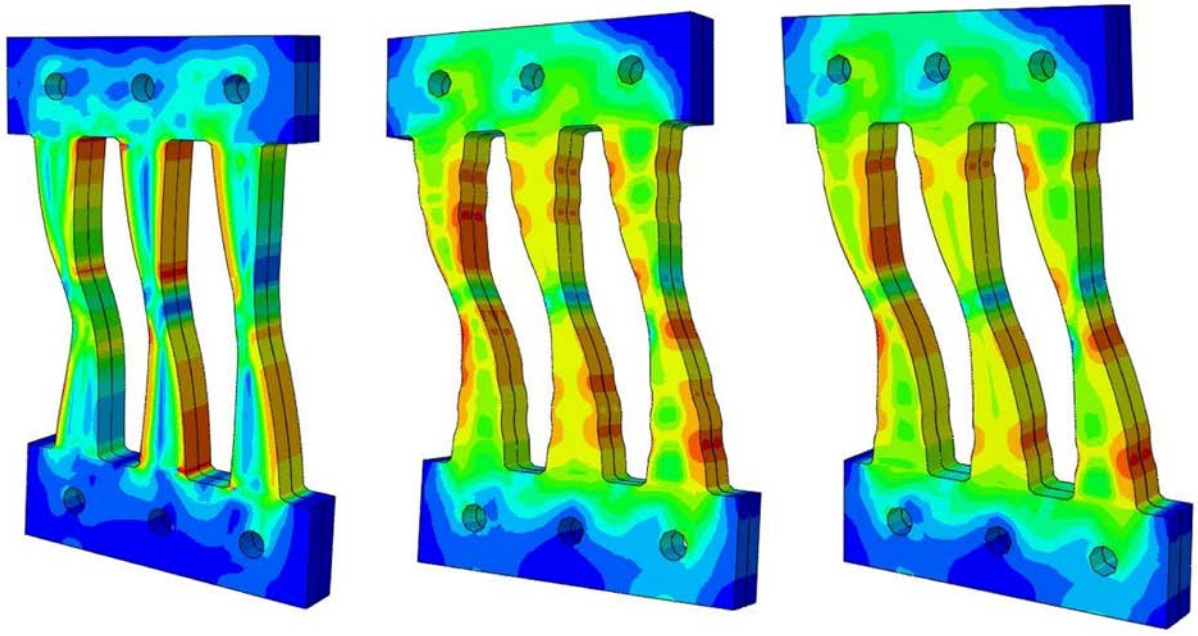

a. Continuous hinge (M_p) b. Four hinges (Coke 4) c. Two hinges (Coke 2)

Fig. 9 – Stress distribution at the target displacement

5. Conclusion

Three different strip dampers proportioned for flexure yielding are studied through a verified finite element analysis model. From the analysis results, the following conclusions can be drawn.

1. The load-displacement hysteresis curve of all the specimens is stable up to the target displacement with a total cumulative displacement of over 2000 mm.
2. Compared to the Coke models, the full-length yielding model sustained more loading cycles before failure.
3. From the stress contours of the finite element analysis, it can be concluded that plastic hinges develop at the radius cut segments of the Coke strip dampers inline with the design concept.
4. The initial stiffness, post-yield stiffness, and maximum force of the Coke dampers are higher than that of the full length yielding strip damper. The increase in stiffness and maximum force is due to the added strip width. Among the Coke slit dampers, the initial stiffness, post-yield stiffness, and the maximum force decrease with an increase in the number of plastic hinges.
5. The energy dissipation capacity of the Coke slit dampers is higher than that of the full-length yielding strip damper at all displacements. The Coke models dissipated higher energy due to the increase in the resistance force. However, since the full-length yielding strip damper sustained more number of loading cycles than the Coke strip dampers, the cumulative dissipated energy of the full-length yielding strip damper is higher.
6. At low displacement amplitudes, the Coke models showed higher viscous damping and equivalent damping while the full-length yielding strip damper showed higher viscous and equivalent damping at large displacement amplitudes.

© The 17th World Conference on Earthquake Engineering

6. Acknowledgments

The work presented in this paper is supported by the National Research Foundation of Korea under the grant number NRF-2018R1A4A1026027

7. References

[1] Spencer Jr, B. F., & Nagarajaiah, S. (2003). State of the art of structural control. Journal of structural engineering, 129(7), 845-856.

[2] Saaed, T. E., Nikolakopoulos, G., Jonasson, J. E., & Hedlund, H. (2015). A state-of-the-art review of structural control systems. Journal of Vibration and Control, 21(5), 919-937.

[3] Prucz, J. C., Kokkinos, F., & Spyrakos, C. C. (1988). Advanced joining concepts for passive vibration control. Journal of Aerospace Engineering, 1(4), 193-205.

[4] Ali, H. E. M., & Abdel-Ghaffar, A. M. (1995). Modeling of rubber and lead passive-control bearings for seismic analysis. Journal of Structural Engineering, 121(7), 1134-1144.

[5] Tirca, L. D., Foti, D., & Diaferio, M. (2003). Response of middle-rise steel frames with and without passive dampers to near-field ground motions. Engineering Structures, 25(2), 169-179.

[6] Ibrahim, R. A. (2008). Recent advances in nonlinear passive vibration isolators. Journal of sound and vibration, 314(3-5), 371-452.

[7] Parulekar, Y. M., & Reddy, G. R. (2009). Passive response control systems for seismic response reduction: A state-of-the-art review. International Journal of Structural Stability and Dynamics, 9(01), 151-177.

[8] Martinelli, P., & Mulas, M. G. (2010). An innovative passive control technique for industrial precast frames. Engineering Structures, 32(4), 1123-1132.

[9] Kelly, J. M., Skinner, R. I., & Heine, A. J. (1972). Mechanisms of energy absorption in special devices for use in earthquake resistant structures. Bulletin of NZ Society for Earthquake Engineering, 5(3), 63-88.

[10] Tyler, R. G. (1978). Tapered steel energy dissipators for earthquake resistant structures. Bulletin of the New Zealand National Society for Earthquake Engineering, 11(4), 282-294.

[11] Chan, R. W., & Albermani, F. (2008). Experimental study of steel slit damper for passive energy dissipation. Engineering Structures, 30(4), 1058-1066.

[12] Lee, C. H., Ju, Y. K., Min, J. K., Lho, S. H., & Kim, S. D. (2015). Non-uniform steel strip dampers subjected to cyclic loadings. Engineering Structures, 99, 192-204.

[13] Simulia, D. S. (2017). Abaqus 2017 documentation.

[14] Federal Emergency Management Agency (FEMA). (2007). Interim Testing Protocols for Determining the Seismic Performance Characteristics of Structural and Nonstructural Components, Report No. FEMA-461.

[15] Council, B. S. S. (2000). FEMA 356-Prestandard and Commentary for the Seismic Rehabilitation of Buildings. Washington DC: Federal Emergency Management Agency.

© The 17th World Conference on Earthquake Engineering